

Measurement of Absolute Hadronic Branching Fractions of D Mesons and $e^+e^- \rightarrow D\bar{D}$ Cross Sections at $E_{\text{cm}} = 3773 \text{ MeV}$

Q. He,¹ H. Muramatsu,¹ C. S. Park,¹ W. Park,¹ E. H. Thomsdike,¹ T. E. Coan,²
 Y. S. Gao,² F. Liu,² M. Artuso,³ C. Boulahouache,³ S. Blusk,³ J. Butt,³
 E. Dambasuren,³ O. Dorkhaidav,³ J. Li,³ N. Menaa,³ R. Mountain,³ R. Nandakumar,³
 K. Randrianarivony,³ R. Redjimi,³ R. Sia,³ T. Skwamicki,³ S. Stone,³ J. C. Wang,³
 K. Zhang,³ S. E. Csonka,⁴ G. Bonvicini,⁵ D. Cinabro,⁵ M. Dubrovina,⁵ R. A. Briere,⁶
 G. P. Chen,⁶ J. Chen,⁶ T. Ferguson,⁶ G. Tatishvili,⁶ H. Vogel,⁶ M. E. Watkins,⁶
 J. L. Rosner,⁷ N. E. Adam,⁸ J. P. Alexander,⁸ K. Berkeman,⁸ D. G. Cassel,⁸
 V. Crede,⁸ J. E. Dubosq,⁸ K. M. Ecklund,⁸ R. Ehrlich,⁸ L. Fields,⁸ L. Gibbons,⁸
 B. Gittelman,⁸ R. Gray,⁸ S. W. Gray,⁸ D. L. Hartill,⁸ B. K. Heltsley,⁸ D. Hertz,⁸
 L. Hsu,⁸ C. D. Jones,⁸ J. Kandaswamy,⁸ D. L. Reinick,⁸ V. E. Kuznetsov,⁸
 H. Mahler-Krug,⁸ T. O. Meyer,⁸ P. U. E. Onyisi,⁸ J. R. Patterson,⁸ D. Peterson,⁸
 E. A. Phillips,⁸ J. Pivarski,⁸ D. Riley,⁸ A. Ryd,⁸ A. J. Sado,⁸ H. Schwartho,⁸ X. Shi,⁸
 M. R. Shepherd,⁸ S. Stroiney,⁸ W. M. Sun,⁸ D. Umer,⁸ K. M. Weaver,⁸ T. Wilksen,⁸
 M. Weinberger,⁸ S. B. Athar,⁹ P. Avery,⁹ L. Brevina-Newell,⁹ R. Patel,⁹ V. Potluri,⁹
 H. Stoeck,⁹ J. Yelton,⁹ P. Rubin,¹⁰ C. Cawley,¹¹ B. I. Eisenstein,¹¹ G. D. Gollin,¹¹
 I. Karliner,¹¹ D. Kim,¹¹ N. Lowrey,¹¹ P. Naik,¹¹ C. Sedlack,¹¹ M. Selen,¹¹ J. Williams,¹¹
 J. Wiss,¹¹ K. W. Edwards,¹² D. Besson,¹³ T. K. Pedlar,¹⁴ D. Cronin-Hennessy,¹⁵
 K. Y. Gao,¹⁵ D. T. Gong,¹⁵ J. Hietala,¹⁵ Y. Kubota,¹⁵ T. Klein,¹⁵ B. W. Lang,¹⁵
 S. Z. Li,¹⁵ R. Poling,¹⁵ A. W. Scott,¹⁵ A. Smith,¹⁵ S. Dobbs,¹⁶ Z. Metreveli,¹⁶
 K. K. Seth,¹⁶ A. Tomaradze,¹⁶ P. Zweber,¹⁶ J. Ernst,¹⁷ A. H. Mahmood,¹⁷ H. Severini,¹⁸
 D. M. Asner,¹⁹ S. A. Dytman,¹⁹ W. Love,¹⁹ S. Mehrabyan,¹⁹ J. A. Mueller,¹⁹
 V. Savinov,¹⁹ Z. Li,²⁰ A. Lopez,²⁰ H. Mendez,²⁰ J. Ramirez,²⁰ G. S. Huang,²¹
 D. H. Miller,²¹ V. Pavlunin,²¹ B. Sanghi,²¹ I. P. J. Shipsey,²¹ G. S. Adams,²²
 M. Chasse,²² M. Cravey,²² J. P. Cummings,²² I. Danko,²² and J. Napolitano²²

(CLEO Collaboration)

¹University of Rochester, Rochester, New York 14627

²Southern Methodist University, Dallas, Texas 75275

³Syracuse University, Syracuse, New York 13244

⁴Vanderbilt University, Nashville, Tennessee 37235

⁵Wayne State University, Detroit, Michigan 48202

⁶Carnegie Mellon University, Pittsburgh, Pennsylvania 15213

⁷Enrico Fermi Institute, University of Chicago, Chicago, Illinois 60637

⁸Cornell University, Ithaca, New York 14853

⁹University of Florida, Gainesville, Florida 32611

¹⁰George Mason University, Fairfax, Virginia 22030

¹¹University of Illinois, Urbana-Champaign, Illinois 61801

¹²Carleton University, Ottawa, Ontario, Canada K1S 5B6
and the Institute of Particle Physics, Canada

¹³University of Kansas, Lawrence, Kansas 66045

¹⁴Luther College, Decorah, Iowa 52101

¹⁵University of Minnesota, Minneapolis, Minnesota 55455

¹⁶Northwestern University, Evanston, Illinois 60208

¹⁷State University of New York at Albany, Albany, New York 12222

¹⁸University of Oklahoma, Norman, Oklahoma 73019

¹⁹University of Pittsburgh, Pittsburgh, Pennsylvania 15260

²⁰University of Puerto Rico, Mayaguez, Puerto Rico 00681

²¹Purdue University, West Lafayette, Indiana 47907

²²Rensselaer Polytechnic Institute, Troy, New York 12180

(Dated: April 1, 2005)

Abstract

Using 55.8 pb⁻¹ of e⁺e⁻ collisions recorded at the (3770) resonance with the CLEO-c detector at CESR, we determine absolute hadronic branching fractions of charged and neutral D mesons using a double tag technique. Among measurements for three D⁰ and six D⁺ modes, we obtain reference branching fractions B(D⁰ ! K⁺) = (3.91 ± 0.08 ± 0.09)% and B(D⁺ ! K⁺π⁺) = (9.5 ± 0.2 ± 0.3)%, where the uncertainties are statistical and systematic, respectively. Final state radiation is included in these branching fractions by allowing for additional, unobserved, photons in the final state. Using a determination of the integrated luminosity, we also extract the cross sections (e⁺e⁻ ! D⁰D⁰) = (3.60 ± 0.07^{+0.07}_{-0.05}) nb and (e⁺e⁻ ! D⁺D⁻) = (2.79 ± 0.07^{+0.10}_{-0.04}) nb.

Absolute measurements of hadronic charm meson branching fractions play a central role in the study of the weak interaction because they serve to normalize many D and B meson branching fractions, from which elements of the Cabibbo-Kobayashi-Maskawa (CKM) matrix [1] are determined. For instance, the determination of the CKM matrix element $|V_{cb}|$ from the $B \rightarrow D^0 \pi^0$ decay rate using full D reconstruction requires knowledge of the D meson branching fractions [2]. In this Letter, we present charge-averaged branching fraction measurements of three D^0 and six D^+ decay modes: $D^0 \rightarrow K^+ \pi^-$, $D^0 \rightarrow K^+ \pi^- \pi^0$, $D^0 \rightarrow K^+ \pi^- \pi^+ \pi^-$, $D^+ \rightarrow K^+ \pi^- \pi^0$, $D^+ \rightarrow K^+ \pi^- \pi^+ \pi^-$, $D^+ \rightarrow K_S^0 \pi^+$, $D^+ \rightarrow K_S^0 \pi^+ \pi^0$, $D^+ \rightarrow K_S^0 \pi^+ \pi^+ \pi^-$, and $D^+ \rightarrow K^+ K^0$. Two of these modes, $D^0 \rightarrow K^+ \pi^-$ and $D^+ \rightarrow K^+ \pi^- \pi^0$, are particularly important because essentially all other D^0 and D^+ branching fractions have been determined from ratios to one of these branching fractions [3].

To date, the most precise measurements of hadronic D branching fractions are made with slow-daughter-pion tagging of D mesons from Z^0 decays and from continuum production in e^+e^- interactions at the $(4S)$ [4, 5]. Previously, the MARK III collaboration measured hadronic branching fractions at the $D\bar{D}$ threshold using a double tagging technique which relied on fully-reconstructed $(3770) \rightarrow D\bar{D}$ decays [6, 7]. This technique obviated the need for knowledge of the luminosity or the $e^+e^- \rightarrow D\bar{D}$ production cross section. We employ a similar technique using CLEO-c data, in a sample roughly six times larger than that of MARK III, resulting in precision comparable to the current PDG world averages.

The data sample we analyze was produced in e^+e^- collisions at the Cornell Electron Storage Ring (CESR) and collected with the CLEO-c detector. It consists of 55.8 pb^{-1} of integrated luminosity collected on the (3770) resonance, at a center-of-mass energy $E_{\text{cm}} = 3773 \text{ MeV}$. At this energy, no additional hadrons accompanying the $D\bar{D}$ pairs are produced. Reconstruction of one D or \bar{D} meson (called single tag or ST) tags the event as either $D^0\bar{D}^0$ or $D^+\bar{D}^-$. For a given decay mode i , we measure independently the D and \bar{D} ST yields, denoted by N_i and $N_{\bar{i}}$. We determine the corresponding efficiencies, denoted by ϵ_i and $\epsilon_{\bar{i}}$, from Monte Carlo simulations. Thus, $N_i = \epsilon_i B_i N_{D\bar{D}}$ and $N_{\bar{i}} = \epsilon_{\bar{i}} B_i N_{D\bar{D}}$, where B_i is the branching fraction for mode i , assuming no CP violation, and $N_{D\bar{D}}$ is the number of produced $D\bar{D}$ pairs. Double tag (DT) events are the subset of ST events where both the D and \bar{D} are reconstructed. The DT yield for D mode i and \bar{D} mode j , denoted by N_{ij} , is given by $N_{ij} = \epsilon_{ij} B_i B_j N_{D\bar{D}}$, where ϵ_{ij} is the DT efficiency. As with ST yields, the charge conjugate DT yields and efficiencies, N_{ji} and ϵ_{ji} , are determined separately. Charge conjugate particles are implied, unless referring to ST and DT yields.

The B_i can be determined from the DT yield N_{ij} and the corresponding ST yield N_j via $B_i = [N_{ij}/N_j] / [\epsilon_j/\epsilon_i]$ [$j = ij$]. Similarly, we have $N_{D\bar{D}} = [N_i N_j / N_{ij}] / [\epsilon_{ij}/(\epsilon_i \epsilon_j)]$. Because $\epsilon_{ij} = \epsilon_i \epsilon_j$, the branching fractions thus obtained are nearly independent of the tag mode efficiency, and $N_{D\bar{D}}$ is nearly independent of all efficiencies. We extract branching fractions and $N_{D\bar{D}}$ by combining ST and DT yields with a least squares technique. Although the D^0 and D^+ yields are statistically independent, systematic effects and misreconstruction resulting in crossfeed introduce correlations among their uncertainties. Therefore, we fit D^0 and D^+ parameters simultaneously, including in the χ^2 statistical and systematic uncertainties and their correlations for all experimental inputs [8]. Thus, yields, efficiencies, and backgrounds are treated uniformly, and the statistical uncertainties on B_i and $N_{D\bar{D}}$ include the correlations among N_i , N_j , and N_{ij} . Also, in the above efficiency ratios most systematic uncertainties are correlated between ST and DT efficiencies, so their effects largely cancel.

The CLEO-c detector is a modification of the CLEO III detector [9, 10, 11], in which the silicon-strip vertex detector was replaced with a six-layer vertex drift chamber, whose

wires are all at small stereo angles to the beam axis [12]. The charged particle tracking system, consisting of this vertex drift chamber and a 47-layer central drift chamber [10] operates in a 1.0 T magnetic field, oriented along the beam axis. The momentum resolution of the tracking system is approximately 0.6% at $p = 1 \text{ GeV}/c$. Photons are detected in an electromagnetic calorimeter, composed of 7800 CsI(Tl) crystals [9], which attains a photon energy resolution of 2.2% at $E = 1 \text{ GeV}$ and 5% at 100 MeV. The solid angle coverage for charged and neutral particles of the CLEO-c detector is 93% of 4π . We utilize two particle identification (PID) devices to separate K from π : the central drift chamber, which provides measurements of ionization energy loss (dE/dx), and, surrounding this drift chamber, a cylindrical ring-imaging Cherenkov (RICH) detector [11], whose active solid angle is 80% of 4π . The combined dE/dx -RICH PID system has a pion or kaon efficiency $> 90\%$ and a probability of pions faking kaons (or vice versa) $< 5\%$. The response of the experimental apparatus is studied with a detailed GEANT-based [13] Monte Carlo simulation of the CLEO detector for particle trajectories generated by EvtGen [14] and final state radiation (FSR) predicted by PHOTOS [15]. Simulated events are processed in a fashion similar to data. The data sample's integrated luminosity (\mathcal{L}) is measured using e^+e^- Bhabha events in the calorimeter [16], where the event count normalization is provided by the detector simulation.

Charged tracks are required to be well-measured and to satisfy criteria based on the track quality. They must also be consistent with coming from the interaction point in three dimensions. Pions and kaons are identified by consistency with the expected dE/dx and RICH information, when available. We form π^0 candidates from photon pairs with invariant mass within 3 standard deviations (σ), with $\sigma = 5\{7 \text{ MeV}/c^2$ depending on photon energy and location, of the known π^0 mass. These candidates are then χ^2 kinematically with their masses constrained to the known π^0 mass. The K_S^0 candidates are selected from pairs of oppositely-charged and vertex-constrained tracks having invariant mass within $12 \text{ MeV}/c^2$, or roughly 4.5σ , of the known K_S^0 mass.

We identify D meson candidates by their invariant masses and total energies. We calculate a beam-constrained mass by substituting the beam energy, E_0 , for the measured D candidate energy: $M^2 = E_0^2 - p_D^2$, where p_D is the D candidate momentum. Performing this substitution improves the resolution of M by one order of magnitude, to about $2 \text{ MeV}/c^2$, which is dominated by the beam energy spread. We define $E = E_D - E_0$, where E_D is the sum of the D candidate daughter energies. For final states consisting entirely of tracks, the E resolution is $7\{10 \text{ MeV}$. A π^0 in the final state degrades this resolution by roughly a factor of two. We accept D candidates with M greater than $1.83 \text{ GeV}/c^2$ and with mode-dependent E requirements of approximately 3σ . For both ST and DT modes, we accept at most one candidate per mode per event. In ST modes, the candidate with the smallest E is chosen, while in DT modes, we take the candidate whose average of D and D^* values, denoted by \bar{M} , is closest to the known D mass.

We extract ST and DT yields from M distributions in the samples described above. We perform unbinned maximum likelihood fits in one and two dimensions for ST and DT modes, respectively, to a signal shape and one or more background components. The signal shape includes the effects of beam energy smearing, initial state radiation, the line shape of the (3770) , and reconstruction resolution. The background in ST modes is described by an ARGUS function [17], which models combinatorial contributions. In DT modes, backgrounds can be uncorrelated, where either the D or D^* is misreconstructed, or correlated, where all the final state particles in the event are correctly reconstructed but are mispartitioned among

TABLE I: Single tag data yields and efficiencies and their statistical uncertainties.

D or D Mode	Yield (10^3)	Efficiency (%)
$D^0 \rightarrow K^+ K^-$	5.11 ± 0.07	64.6 ± 0.3
$D^0 \rightarrow K^+ K^-$	5.15 ± 0.07	65.6 ± 0.3
$D^0 \rightarrow K^+ K^- K^0$	9.51 ± 0.11	31.4 ± 0.1
$D^0 \rightarrow K^+ K^- K^0$	9.47 ± 0.11	31.8 ± 0.1
$D^0 \rightarrow K^+ K^- K^+ K^-$	7.44 ± 0.09	43.6 ± 0.2
$D^0 \rightarrow K^+ K^- K^+ K^-$	7.43 ± 0.09	43.9 ± 0.2
$D^+ \rightarrow K^+ K^- K^0$	7.56 ± 0.09	50.7 ± 0.2
$D^+ \rightarrow K^+ K^- K^0$	7.56 ± 0.09	51.3 ± 0.2
$D^+ \rightarrow K^+ K^- K^+ K^-$	2.45 ± 0.07	25.7 ± 0.2
$D^+ \rightarrow K^+ K^- K^+ K^-$	2.39 ± 0.07	25.7 ± 0.2
$D^+ \rightarrow K_S^0 K^- K^0$	1.10 ± 0.04	45.5 ± 0.4
$D^+ \rightarrow K_S^0 K^- K^0$	1.13 ± 0.04	45.9 ± 0.4
$D^+ \rightarrow K_S^0 K^- K^+ K^-$	2.59 ± 0.07	22.4 ± 0.2
$D^+ \rightarrow K_S^0 K^- K^+ K^-$	2.50 ± 0.07	22.4 ± 0.2
$D^+ \rightarrow K_S^0 K^- K^+ K^-$	1.63 ± 0.06	31.1 ± 0.2
$D^+ \rightarrow K_S^0 K^- K^+ K^-$	1.58 ± 0.06	31.3 ± 0.2
$D^+ \rightarrow K^+ K^- K^+ K^-$	0.64 ± 0.03	41.4 ± 0.5
$D^+ \rightarrow K^+ K^- K^+ K^-$	0.61 ± 0.03	40.8 ± 0.5

the D^0 and D^+ . In fitting the two-dimensional $M(D^0)$ versus $M(D^+)$ distribution, we model the uncorrelated background by a pair of functions, where one dimension is an ARGUS function and the other is the signal shape. We model the correlated background by an ARGUS function in $M(D^0)$ and a Gaussian in the orthogonal variable, which is $|M(D^0) - M(D^+)| = 2$.

Table I gives the 18 ST data yields and efficiencies determined from simulated events. Figure 1 shows the $M(D)$ distributions for the nine decay modes with D^0 and D^+ candidates combined. Overlaid are the fitted signal and background components. We also measure 45 DT yields in data and determine the corresponding efficiencies from simulated events. Figure 2 shows $M(D)$ for all modes combined, separated by charge. We find total DT yields of 2484 ± 51 for D^0 and 1650 ± 42 for D^+ . Because of the cleanliness of the DT modes, their statistical yield uncertainties are close to $\sqrt{N_{ij}}$.

Using a missing mass technique, we measure efficiencies for reconstructing tracks, K_S^0 decays, and K^0 decays in both data and simulated events. We fully reconstruct $(3770) \rightarrow D D^*, (2S) \rightarrow J/\psi K^+ K^-$, and $(2S) \rightarrow J/\psi K^0 K^0$ events, leaving out one particle, for which we wish to determine the efficiency. The missing mass of this combination peaks at the mass of the omitted particle, whether or not it is detected. Then, the desired efficiency is the fraction of this peak with this particle correctly reconstructed. For tracks and K_S^0 candidates, we find good agreement between efficiencies in data and simulated events. For K^0 candidates, we correct the simulated efficiencies by 3.9%, which is the level of disagreement with data found in this study. The relative uncertainties in these determinations, 0.7% per track, 3.0% per K_S^0 , and 2.0% per K^0 , are the largest contributions to the systematic uncertainties.

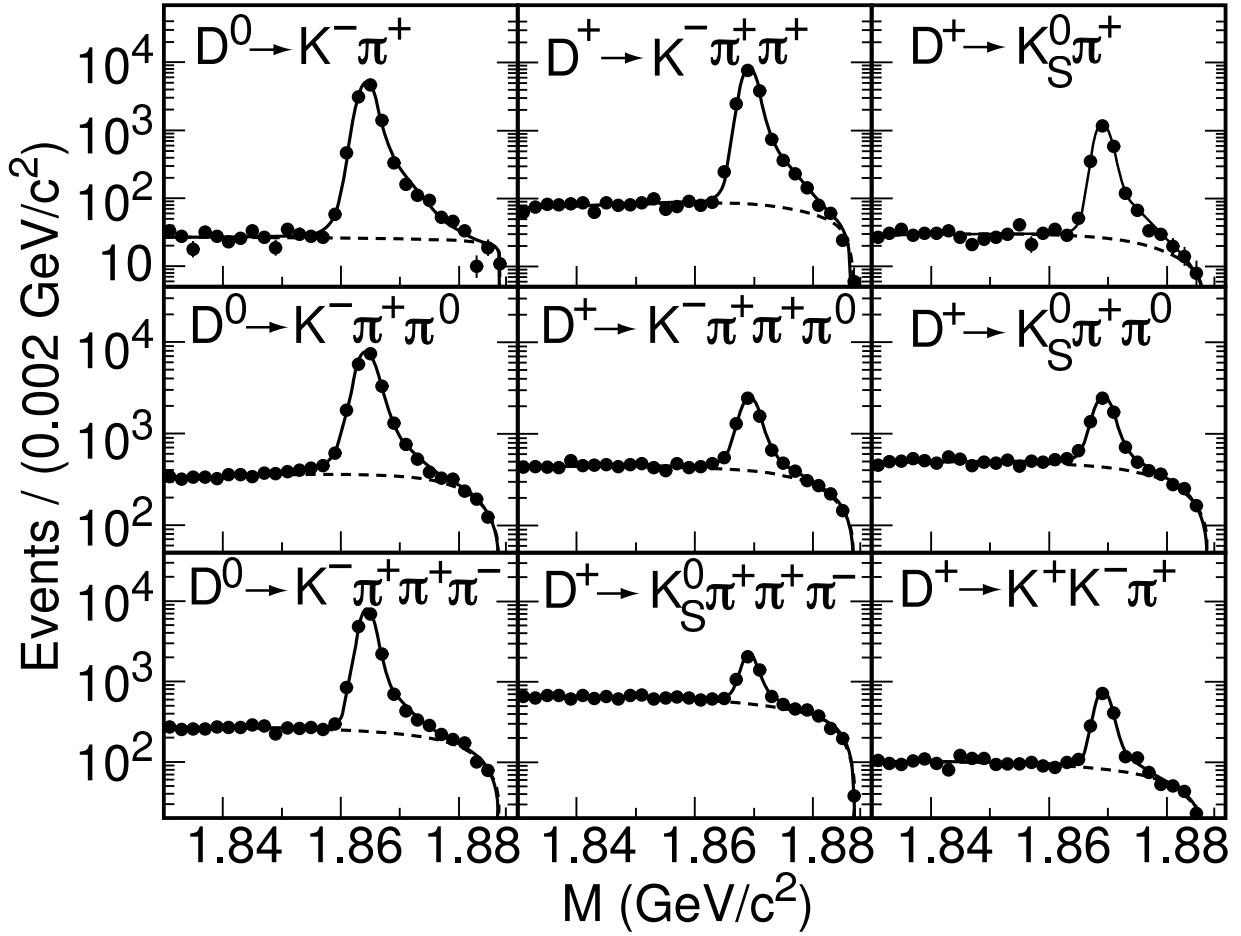


FIG. 1: Semilogarithmic plots of ST yields and fits, with D^0 and D^+ combined for each mode. Data are shown as points with error bars. The solid lines show the total fits and the dashed lines the background shapes. The high mass tails on the signal are due to initial state radiation.

We study the simulation of the PID efficiencies using decays with unambiguous particle content, such as $D^0 \rightarrow K_S^0 \pi^+$ and $D^+ \rightarrow K^- \pi^+ \pi^+$. We find a need to correct the simulated efficiencies by 0.3% for π^+ and 1.3% for K^- , and we apply associated systematic uncertainties of the same size. Other sources of efficiency uncertainty include: the E requirements (1.0{2.5%}), for which we examine E sidebands; modeling of particle multiplicity and detector noise (0.2{1.3%}); and modeling of resonant substructure in multi-body modes (0.4{1.5%}), which we assess by comparing simulated momentum spectra to those in data. We also include additive uncertainties of 0.5% to account for variations of yields with fit function. Smaller systematic uncertainties arise from online and offline filtering (0.4%), simulation of FSR (0.5% per D^0 or D^+), and the assumed width of the (3770) in the M signal shape (0.6%). The effect of quantum correlations between the D^0 and \bar{D}^0 states appears through D^0 - \bar{D}^0 mixing and through doubly Cabibbo-suppressed decays [18]. The former contribution is limited by available measurements [3] to be less than $O(10^{-3})$ and is, therefore, neglected in this analysis. The latter contribution is addressed with a systematic uncertainty due to the unknown phase of interference in neutral DT modes between the Cabibbo-favored amplitude and the amplitude for doubly Cabibbo-suppressed transitions in

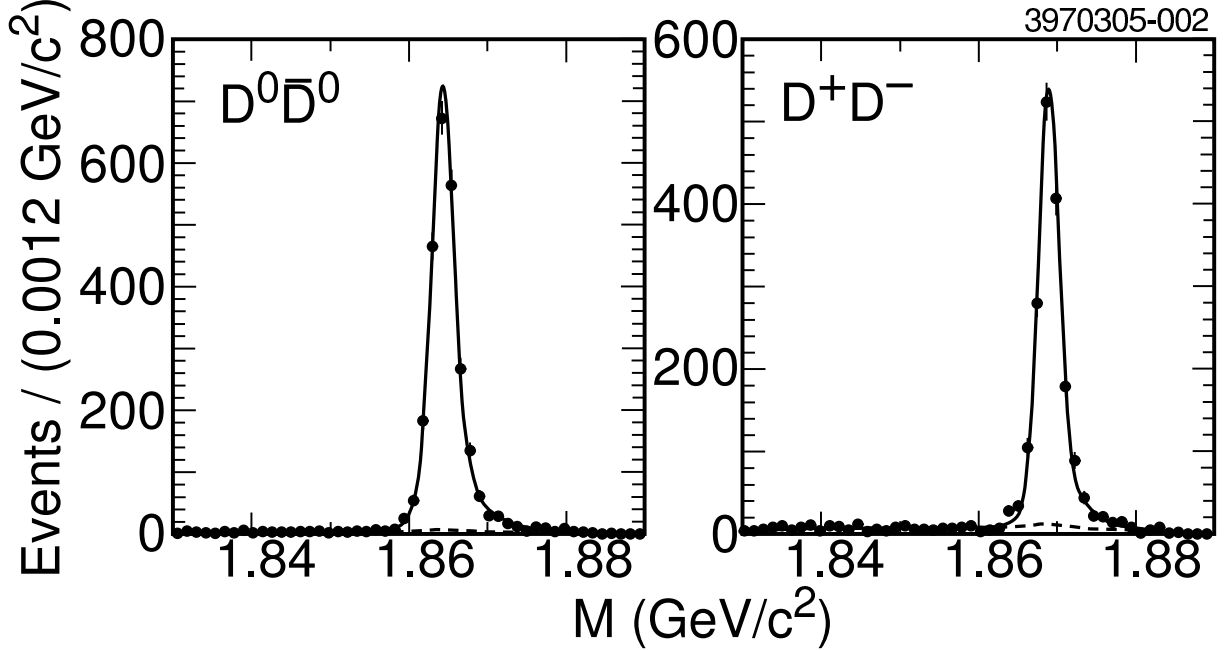


FIG. 2: $D^0 D^0$ yields and fits projected onto the D^0 and D^+ axes and summed over all modes. Data are shown as points with error bars. The solid lines show the total fit and the dashed lines the background shapes.

both D^0 and D^0 (0.8%).

The branching fraction fitter [8] takes these systematic uncertainties as input, along with ST and DT yields and efficiencies, crossfeed probabilities among the modes, background branching fractions and efficiencies, and statistical uncertainties on all of these measurements. The estimated crossfeed and background contributions produce yield adjustments of 0.1%. Their dependence on the fit parameters is taken into account both in the yield subtraction and in the χ^2 minimization. We validated the analysis technique, including the branching fraction fit, by studying simulated $D D$ events in a sample 50 times the size of our data sample. We reproduced the input branching fractions with biases due to our procedures that were less than one-third of the statistical errors on the data and consistent with zero.

The results of the data fit are shown in Table II. The χ^2 of the fit is 28.1 for 52 degrees of freedom, corresponding to a confidence level of 99.7%. To obtain the separate contributions from statistical and systematic uncertainties, we repeat the fit without any systematic inputs and take the quadrature difference of uncertainties. All nine branching fractions are consistent with, and most are higher than, the current PDG averages [3]. In the D candidate reconstruction, we do not explicitly search for FSR photons. However, because FSR is simulated in the samples used to calculate efficiencies, our measurements represent inclusive branching fractions for signal processes with any number of photons radiated from the final state particles. If no FSR were included in the simulations, then all the branching fractions would change by ϵ_{FSR} in Table II.

The correlation coefficient, ρ , between $N_{D^0 D^0}$ and $N_{D^+ D^+}$ is 0.07, and each is essentially uncorrelated with branching fractions of the other charge. Correlations among branching fractions are in the range 0.2–0.7. In the absence of systematic uncertainties, there would be almost no correlation between the charged and neutral D parameters.

TABLE II: Fitted branching fractions and $D\bar{D}$ pair yields, along with the fractional FSR corrections and comparisons to the Particle Data Group [3]’s results. Uncertainties are statistical and systematic, respectively.

D Decay Mode	Fitted B (%)			PDG B (%)			FSR
K^+	3.91	0.08	0.09	3.80	0.09		2.0%
$K^+ 0$	14.9	0.3	0.5	13.0	0.8		0.8%
$K^+ +$	8.3	0.2	0.3	7.46	0.31		1.7%
$K^+ + +$	9.5	0.2	0.3	9.2	0.6		2.2%
$K^+ + + 0$	6.0	0.2	0.2	6.5	1.1		0.6%
$K_S^0 +$	1.55	0.05	0.06	1.41	0.10		1.8%
$K_S^0 + 0$	7.2	0.2	0.4	4.9	1.5		0.8%
$K_S^0 + +$	3.2	0.1	0.2	3.6	0.5		1.4%
$K^+ K^+$	0.97	0.04	0.04	0.89	0.08		0.9%
D D Yield		Fitted Value				FSR	
$N_{D^0\bar{D}^0}$		(2.01	0.04	0.02)	10^5	0.2%	
$N_{D^+\bar{D}^-}$		(1.56	0.04	0.01)	10^5	0.2%	

TABLE III: Fitted ratios of branching fractions to the reference branching fractions $R_0 = B(D^0 \rightarrow K^+ \pi^-) / B(D^0 \rightarrow K^+ \pi^-)$ and $R_+ = B(D^+ \rightarrow K^+ \pi^0) / B(D^+ \rightarrow K^+ \pi^0)$, along with the fractional FSR corrections and comparisons to the Particle Data Group [3]’s results. Uncertainties are statistical and systematic, respectively.

D Decay Mode	Fitted B=R ₀₌₊			PDG B=R ₀₌₊			FSR
$K^+ 0$	3.65	0.05	0.11	3.42	0.22		+1.2%
$K^+ +$	2.10	0.03	0.06	1.96	0.08		+0.3%
$K^+ + + 0$	0.613	0.013	0.019	0.70	0.12		+1.7%
$K_S^0 +$	0.165	0.004	0.006	0.153	0.003		+0.4%
$K_S^0 + 0$	0.752	0.016	0.033				+1.4%
$K_S^0 + +$	0.340	0.009	0.014	0.39	0.05		+0.8%
$K^+ K^+$	0.101	0.004	0.002	0.097	0.006		+1.3%

We also compute ratios of branching fractions to the reference branching fractions, shown in Table III. These ratios have higher precision than the individual branching fractions, and they also agree with the PDG averages. Without FSR corrections to the efficiencies, all seven ratios would be 0.3% to 1.7% higher.

We obtain the $e^+e^- \rightarrow D\bar{D}$ cross sections by scaling $N_{D^0\bar{D}^0}$ and $N_{D^+\bar{D}^-}$ by the luminosity, which we determine to be $L = (55.8 \pm 0.6) \text{ pb}^{-1}$. Thus, at $E_{\text{cm}} = 3773 \text{ MeV}$, we find peak cross sections of $(e^+e^- \rightarrow D^0\bar{D}^0) = (3.60 \pm 0.07^{+0.07}_{-0.05}) \text{ nb}$, $(e^+e^- \rightarrow D^+\bar{D}^-) = (2.79 \pm 0.07^{+0.10}_{-0.04}) \text{ nb}$, $(e^+e^- \rightarrow D\bar{D}) = (6.39 \pm 0.10^{+0.17}_{-0.08}) \text{ nb}$, and $(e^+e^- \rightarrow D^0\bar{D}^0) = 0.776 \pm 0.024^{+0.014}_{-0.006}$, where the uncertainties are statistical and systematic, respectively. In addition to the systematic uncertainties on $N_{D^0\bar{D}^0}$, $N_{D^+\bar{D}^-}$, and the luminosity, the cross section systematic uncertainties also include the effect of E_{cm} vari-

ations with respect to the peak. We account for the correlation between the charged and neutral cross sections in computing the uncertainty on the total cross section. Our measured cross sections are in good agreement with BES [19] and higher than those of MARK III [7].

In summary, we report measurements of three D^0 and six D^+ branching fractions and the production cross sections ($D^0 D^0$), ($D^+ D^-$), and ($D D$) using a sample of 55.8 pb^{-1} of $e^+e^- \rightarrow D D$ data obtained at $E_{\text{cm}} = 3773 \text{ MeV}$. We find branching fractions in agreement with, but somewhat higher, than those in the PDG [3] summary. We note that, unlike the branching fractions used in the PDG averages, our measurements are corrected for FSR. Not doing so would lower our branching fractions by 0.6% to 2.2%. With our current data sample, the statistical and systematic uncertainties are of comparable size. Many of the systematic uncertainties, such as those for tracking and particle identification efficiencies, will be improved with larger data samples.

We gratefully acknowledge the effort of the CESR staff in providing us with excellent luminosity and running conditions. This work was supported by the National Science Foundation and the U.S. Department of Energy.

-
- [1] M. Kobayashi and T. Maskawa, *Prog. Theor. Phys.* **49**, 652 (1973).
 - [2] See review by M. Artuso and E. Barberio in Ref. [3].
 - [3] S. Eidelman et al. (Particle Data Group), *Phys. Lett. B* **592**, 1 (2004).
 - [4] R. Barate et al. (ALEPH Collaboration), *Phys. Lett. B* **403**, 367 (1997).
 - [5] D. S. Akerib et al. (CLEO Collaboration), *Phys. Rev. Lett.* **71**, 3070 (1993).
 - [6] R. M. Baltusaitis et al. (MARK III Collaboration), *Phys. Rev. Lett.* **56**, 2140 (1986).
 - [7] J. Adler et al. (MARK III Collaboration), *Phys. Rev. Lett.* **60**, 89 (1988).
 - [8] W. M. Sun, physics/0503050 [*Nucl. Instrum. Methods Phys. Res., Sec. A* (to be published)].
 - [9] Y. Kubota et al. (CLEO Collaboration), *Nucl. Instrum. Methods Phys. Res., Sec. A* **320**, 66 (1992).
 - [10] D. Peterson et al., *Nucl. Instrum. Methods Phys. Res., Sec. A* **478**, 142 (2002).
 - [11] M. Artuso et al., *Nucl. Instrum. Methods Phys. Res., Sec. A* **502**, 91 (2003).
 - [12] R. A. Briere et al. (CLEO-c/CESR-c Taskforces & CLEO-c Collaboration), Cornell LEPP preprint CLNS 01/1742 (2001).
 - [13] Computer code GEANT 3.21 in R. Brun et al., CERN Report No. W 5013 (unpublished).
 - [14] D. J. Lange, *Nucl. Instrum. Methods Phys. Res., Sec. A* **462**, 152 (2001).
 - [15] E. Barberio and Z. Was, *Comput. Phys. Commun.* **79**, 291 (1994).
 - [16] G. Crawford et al. (CLEO Collaboration), *Nucl. Instrum. Methods Phys. Res., Sec. A* **345**, 429 (1994).
 - [17] H. Albrecht et al. (ARGUS Collaboration), *Phys. Lett. B* **241**, 278 (1990).
 - [18] D. M. Asner and W. M. Sun, hep-ph/0507238, submitted to *Phys. Rev. D*.
 - [19] M. Ablikim et al. (BES Collaboration), *Phys. Lett. B* **603**, 130 (2004).